

Effect of hypericin-mediated photodynamic therapy on the expression of vascular endothelial growth factor in human nasopharyngeal carcinoma

RAMASWAMY BHUVANESWARI¹, YAP YIK-YUEN GAN², KAREN KAR LYE YEE¹,
KHEE CHEE SOO¹ and MALINI OLIVO¹

¹National Cancer Centre Singapore, 11 Hospital Drive, Singapore 169610; ²Natural Sciences and Science Education, National Institute of Education, Nanyang Technological University, 1 Nanyang Walk, Singapore 637616

Received April 23, 2007; Accepted June 1, 2007

Abstract. Photodynamic therapy (PDT) is currently being used as an alternative treatment modality for various types of cancers. PDT involves the selective uptake and retention of a photosensitizer in the tumor followed by light irradiation of an appropriate wavelength to cause the destruction of tumor cells by the formation of cytotoxic reactive oxygen species. The photosensitizer, hypericin, has shown great potential due to its light-dependent tumor destructive properties. However, as hypericin-mediated PDT primarily targets tumor vasculature, it induces certain pro-angiogenic factors such as vascular endothelial growth factor (VEGF) in the tumor tissue as a result of hypoxia. This study examines the role of hypericin-mediated photodynamic therapy in stimulating the expression of key angiogenesis growth factor VEGF in order to elucidate the process of tumor angiogenesis in nasopharyngeal carcinoma xenografts. We also investigated the effect of angiogenesis inhibitor celebrex on human VEGF levels when combined with hypericin-PDT. These studies were conducted on an *in vivo* human nasopharyngeal xenograft model. VEGF was measured in the control and hypericin-PDT treated tumors. VEGF levels were found to be higher when the tumors were treated at a 1-h drug-light interval compared to a 6-h interval, due to extensive vascular damage. At 72 h post hypericin-PDT, VEGF levels were upregulated indicating the initiation of regrowth in tumors. The use of angiogenesis inhibitor, celebrex, along with hypericin-PDT downregulated the human VEGF levels suggesting that angiogenesis inhibitors can be used to improve the outcome of hypericin-PDT in nasopharyngeal carcinomas.

Introduction

Photodynamic therapy (PDT) involves the administration of a tumor-localizing photosensitizing drug, which is activated by light of a specific wavelength in the presence of molecular oxygen thus generating reactive oxygen species that are toxic to the tumor (1). PDT is currently being considered as an attractive alternative treatment for various superficial cancers (2). To a great extent, the efficacy of PDT depends on the selection of the photosensitizer based on its intratumoral accumulation and phototoxicity to cancer cells. One such promising second-generation photosensitizer is hypericin, a hydroxylated phenanthroperylenequinone (Fig. 1) obtained from *Hypericum perforatum* (St. John's Wort) plants currently being studied for photodynamic diagnosis and therapy applications (3). The primary action of hypericin-PDT is damage to the tumor vasculature rather than direct killing of tumor cells (4). In clinical trials, we have reported the use of hypericin as a prognostic marker for the diagnosis of bladder cancer (5).

Photodynamic therapy is an oxygen-consuming modality, and an inherent consequence of PDT is local hypoxia. This condition arises either due to direct oxygen consumption during treatment or indirectly due to the destruction of tumor vasculature as a result of effective treatment (6). Some areas in the tumor may receive suboptimal PDT due to the limited penetration depth of light in tissue and the nonhomogeneous distribution of the photosensitizer within the tumor. As a result, cells under hypoxic stress may switch to an adaptive response by inducing a hypoxia-inducible factor such as HIF-1 α thus triggering angiogenesis.

Angiogenesis is the formation of new blood vessels from pre-existing vessels. It is a vital process in the progression of cancer from small, localized neoplasms to larger, growing, and potentially metastatic tumors (7). Therefore, the process of tumor angiogenesis is triggered by the tumor's release of pro-angiogenic signals such as VEGF, which bind to receptors on nearby vessel endothelial cells. Vascular endothelial growth factor is a potent regulator of tumor angiogenesis that plays a critical role by increasing blood vessel permeability, endothelial cell growth, proliferation, migration and differentiation (8). It is upregulated in response to hypoxic

Correspondence to: Dr Malini Olivo, National Cancer Centre Singapore, 11 Hospital Drive, Singapore 169610
E-mail: dmsmcd@nccs.com.sg

Key words: hypericin, photodynamic therapy, angiogenesis, vascular endothelial growth factor, nasopharyngeal carcinoma

conditions in the tumor via the transcription of hypoxia-inducible factor (HIF-1 α) (9). Cellular and circulating levels of VEGF have been elevated in haematological malignancies and are adversely associated with prognosis (10).

Nasopharyngeal carcinoma (NPC) is a tumor arising from the epithelial cells that line the nasopharynx. Although treatment outcomes for NPC have substantially improved, there is still a need for reducing treatment failure for patients with advanced disease (11). In view of the side effects of radiotherapy and chemotherapy and the high failure rate for advanced disease, PDT has been explored as a possible alternative modality of treatment for NPC. PDT has shown promise in treating recurrent nasopharyngeal carcinoma, and also combining PDT with chemotherapy seems to prolong the survival time of the patients (12). Detection of VEGF has shown potential as a tumor marker for the early diagnosis of metastatic NPC (13), and studies have also indicated poor prognosis for NPC patients with higher serum VEGF levels compared to levels in the serum of healthy individuals (14). Several lines of evidence have implicated VEGF in tumorigenesis, and understanding the role of VEGF in tumor angiogenesis has facilitated the development of novel targeting agents that specifically interfere with angiogenesis (15).

Upregulation of various angiogenic factors such as VEGF, HIF-1 α , COX-2, bFGF, MMPs, has been reported in tumors treated with PDT (16,17). Studies by our group have shown the upregulation of HIF-1 α , VEGF, COX-2 and bFGF in hypericin-mediated PDT-treated tumors, suggesting that PDT-induced damage to tumor microvasculature and the resultant hypoxia upregulated the expression of certain pro-angiogenic factors (18). We also reported that the inclusion of various angiogenic inhibitors along with PDT treatment enhanced the PDT effectiveness. Currently, anti-angiogenesis agents are being developed to target different growth factors and molecular pathways that play a major role in tumor angiogenesis. The administration of celebrex along with hypericin-PDT has shown improvement in the overall tumor response in human nasopharyngeal xenografts (17).

The aim of this study was to evaluate the impact of hypericin-mediated PDT on tumor angiogenesis in relation to the expression of the key angiogenesis growth factor VEGF in nasopharyngeal carcinoma. Fluorescence image analysis was performed to determine the optimal drug-light interval for conducting hypericin-PDT experiments. Also, angiogenesis inhibitor celebrex which is a selective cyclooxygenase-2 (COX-2) inhibitor and a non-steroidal anti-inflammatory drug (NSAID) was used in combination with hypericin-mediated PDT to investigate its effect on the expression of VEGF.

Materials and methods

Drug preparation. A stock solution of hypericin from Molecular Probes Inc., USA, was prepared by adding 200 μ l of dimethyl sulfoxide, DMSO (Sigma Aldrich Inc., St. Louis MO, USA) to 1 mg of hypericin. A working concentration of 5 mg/kg was prepared by further dilution with phosphate-buffered saline (PBS).

Murine xenograft tumor model. Nasopharyngeal carcinoma cell line HK1 was used for the VEGF studies, and CNE-2

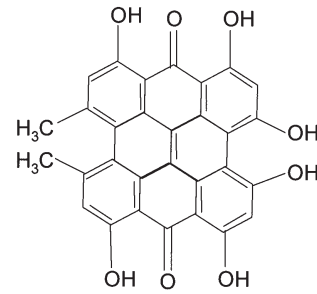


Figure 1. Chemical structure of hypericin, a hydroxylated phenanthroperylenequinone.

cells were used to study the anti-angiogenesis effects of celebrex. The cells were grown in culture medium RPMI-1640 supplemented with 10% fetal bovine serum (FBS; Hyclone, Logan, UT), 1X L-glutamine, 100 units/ml penicillin and streptomycin (Gibco) and 1X sodium pyruvate in an atmosphere of 5% CO₂ at 37°C. Once confluent, the cells were washed with 1X phosphate-buffered saline and trypsinized with 0.05% Trypsin-EDTA (Gibco). The cells were then re-suspended in Hank's balanced salt solution (HBSS) (Gibco BRL, USA). A cell suspension of 1.5x10⁶ was prepared in HBSS and a volume of 100 μ l was injected subcutaneously into the flanks of 6-8 weeks male balb/c nude mice (Animal Resource Centre, Perth, Australia). PDT was performed when tumors reached 6-7 mm in diameter and estimated by using the formula; volume = ($\pi/6$ x d1 x d2 x d3); where d1, d2 and d3 are tumor dimensions in 3 orthogonal directions. The animals were housed in a licensed biomedical research facility, and all procedures were carried out under the approval of the Institutional Animal Care and Use Committee (IACUC) of the National Cancer Centre Singapore.

Fluorescence imaging and data analysis. A dose of 5 mg/kg of hypericin was administered to mice through tail vein injections. Mice were anesthetized at 1-h and 6-h time points using 1:1 vol/vol cocktail of ketamine hydrochloride (Trittau, Germany) and valium (David Bull Laboratories, Australia). The skin overlying the tumor was carefully removed to expose the tumor. A fluorescence endoscope system (Karl Storz, Tuttlingen, Germany) was used to perform macroscopic fluorescence digital imaging of the mouse tumors. The endoscope system was interfaced to a computer in order to store the images immediately. The endoscope system consisted of a xenon arc lamp filtered by a band pass filter (370-450 nm) and a sensitive color CCD video camera with a long pass filter (cut-off wavelength at 560 nm). The instrumentation of the digitized fluorescence imaging system has been extensively described in Zheng *et al.* (19). Image analysis was performed by quantifying the red and blue intensities of the images using the Microimage software [Olympus Optical Co (Europa), Germany]. The red channel registered the fluorescence of the photosensitizer. Based on this, the red to blue ratio was calculated to understand the uptake kinetics of the photosensitizer.

Photodynamic treatment for VEGF estimation. Hypericin prepared in dimethyl sulfoxide (DMSO) and phosphate-

 SPANDIDOS PUBLICATIONS solution (PBS), was injected intravenously into the of the animals at a dose of 5 mg/kg body weight.

The animals were kept under conditions of subdued lighting until commencement of PDT. A filtered halogen light source (Zeiss KL1500) was fitted with a customized 560- to 640-nm band pass filter. After the drug-light interval of 6 h, the animals were anesthetized with a 1:1 cocktail of ketamine hydrochloride and valium. Thereafter the tumors were exposed to light at a dose of 120 J/cm² fluence and 50 mW/cm² fluence rate. Control and experimental groups of 24, 48 and 72 h post PDT were compared. Eight animals were assigned to each group in order to measure the VEGF levels.

Tumor tissue lysate preparation. Animals were sacrificed at 24, 48 and 72 h post PDT. At the designated time points, the mice were anaesthetized with a cocktail of hypnorm (Janssen Pharmaceutical, Belgium), dormicum (David Bull Laboratories, Australia) and deionized water (1:1:2 vol/vol). Cardiac puncture was performed to collect blood at various time points. The cardiac puncture is a one-off procedure for each animal. After withdrawing the blood from the heart, the mice were sacrificed by cervical dislocation before harvesting the tumor tissue. Tissue lysate buffer (T-PER, Pierce) containing protease inhibitor (Complete Mini, Roche) was added to the tissue sample before homogenization to obtain the tissue lysate.

Estimation of mouse and human VEGF using enzyme-linked immunosorbent assay (ELISA). Mouse and human VEGF were detected using ELISA kits (Human VEGF ELISA kit and Mouse VEGF ELISA kit; RayBiotech Inc., USA). The materials provided in the kit consisted of capture antibody, detection antibody, a standard solution and streptavidin-HRP. The assay was run as summarized in the general ELISA protocol on 96-well microplates. Optical density was determined using a microplate reader set at a wavelength of 450 nm (Sunrise™ Tecan, Switzerland). VEGF concentration was read using a standard curve and was recorded in pg/ml.

Protocol for anti-angiogenesis treatment with celebrex. The light dose was delivered with a 360-W, 82-V halogen photo-optic lamp (Osram Corp., KY, USA). The output of filtered light was measured with a power meter (Coherent Inc., CA, USA). Tumors were exposed to a total light dose of 42.4 J/cm². Hypericin was administered at a dose of 2 mg/kg. Celebrex, a COX-2 inhibitor, was purchased from Pharmacia Pfizer, Puerto Rico. Every 200 mg of celebrex capsule was weighed and extracted with 1 ml of DMSO overnight in an orbital shaker (Forma Scientific, OH, USA) at 40°C, 250 rpm. The celebrex solution was spun down at 1800 rpm for 10 min at 25°C, and the supernatant was sterilized by filtering it through a 0.2-μM acetate filter (Schleicher & Schuell, Dassel, Germany). A total of 5 groups, n=10, were studied. These included the control, the hypericin-PDT-treated only group, the celebrex-only group, and the groups administered an initial dose of celebrex at 6 h post hypericin-PDT and an initial dose of celebrex at 24 h post hypericin-PDT. Mice were administered a daily dose of 15 mg/kg of celebrex intraperitoneally. Tumors were collected 24 days post PDT to perform further experiments.

RNA isolation. Tumor tissue weighing 50-150 mg was homogenized with DiAx 900 homogenizer (Heidolph, Schwabach, Germany) in 1 ml of TRIzol (Invitrogen). The homogenate was incubated at room temperature for 5 min before centrifugation at 12000 x g for 10 min at 4°C. The supernatant was transferred to a fresh tube, 100 μl of 1-bromo-3-chloropropane (Sigma Aldrich) was added and vortexed vigorously for 15 sec. The homogenate was further allowed to incubate at room temperature for 5 min before centrifuging for 15 min at 4°C, 12000 x g. Ribonucleic acid located in the colorless upper aqueous phase was isolated and transferred to a fresh tube containing 0.5 ml of 2-propanol (Merck) for every milliliter of TRIzol initially used. This mixture was vortexed and incubated at room temperature for 5 min before centrifuging at 12000 x g for 5 min at 4°C. The supernatant was removed, the RNA pellet was washed with 1 ml of 70% ethanol for every milliliter of TRIzol initially used, and the pellet was vortexed and centrifuged at 7500 x g for 5 min at 4°C. Subsequently, the RNA pellet was air-dried and dissolved in 20-30 μl of diethyl pyrocarbonate (DEPC) (Sigma Aldrich)-treated water, and the dissolved RNA was heated for 5 min at 60°C. Ribonucleic acid quality was determined by running RNA samples in 1% agarose gel (Sea Kem LEAgarose, FMC Bio Products, ME, USA) in Tri/acetic acid/EDTA (TAE) buffer (Bio-Rad Laboratories, CA, USA). With every 50 ml of agarose, 20 μl of ethidium bromide (Bio-Rad Laboratories) was added. A working concentration of RNA sample (3 μl) was added to 1 μl of 6X blue/orange loading dye and diluted with 2 μl of DEPC-treated water.

cDNA synthesis. In each sample of complimentary deoxy-ribonucleic acid (cDNA) that was synthesized, 2 μg of RNA, 500 ng/μl oligodT (15) primer (1st Base, Singapore Science Park II, Singapore) and 0.01 mM polymerase chain reaction (PCR) nucleotide mix (Promega, Madison, WI, USA) were utilized. This solution was mixed well and incubated for 5 min at 65°C. Then the mixture was cooled on ice for 2 min. Subsequently, a cocktail solution was constituted using 4 μl of 5X first-strand buffer, 0.2 mM dithiothreitol (DTT) (Invitrogen Life Technologies, CA, USA), and 40 units of recombinant RNasin® ribonuclease inhibitor (Promega), and the cocktail mixture was fixed to 10 μl per sample with DEPC-treated water before adding to the individual sample. The mixture was mixed well and incubated for 50 min at 45°C. The reverse-transcribed samples containing cDNA were heated for 15 min at 75°C, hence inactivating the recombinant RNasin ribonuclease inhibitor.

Reverse transcription-polymerase chain reaction (RT-PCR). The primer sequence design was a kind gift from the Brain Tumor Research Laboratory of the National Cancer Centre Singapore (Table I). All primers were synthesized by 1st Base. The reverse transcription-polymerase chain reaction mixture in each sample consisted of 1 μl of cDNA, 2.5 μl of thermophilic DNA polymerase, 10X magnesium-free buffer, 39.5 μM magnesium chloride solution, 10 μM of PCR nucleotide mix, 10 pmol/μl of respective premixed forward and reverse primers and 1.25 units of TaqDNA polymerase in storage buffer B (Promega). The reactive mixture in each sample was

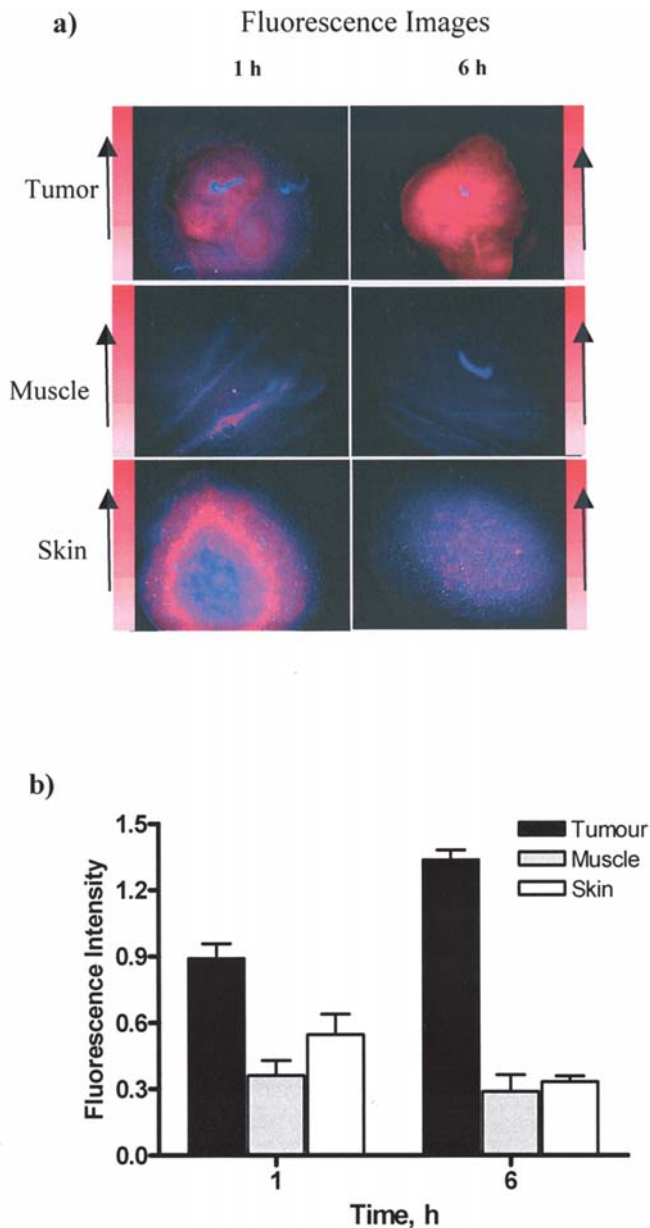


Figure 2. (a) Representative red fluorescence images of tumor, muscle and skin at 1 and 6 h post hypericin administration. (b) Uptake kinetics of hypericin in tumor, muscle and skin at 1 and 6 h post intravenous administration tabulated from fluorescence images captured using Karl Storz Fluorescence Endoscopy System. Each group represents the mean (bars, SE) of five tumors.

fixed to a 25- μ l volume with milliQ water and then mixed well, and RT-PCR was performed in a PTC-100™ programmable thermal controller (MJ Research Inc., MA, USA). The RT-PCR amplification process was conducted over 35 cycles. The first cycle consists of denaturation of cDNA for 2.5 min at 94°C, followed by annealing at 55°C for 30 sec and elongation at 72°C for 1 min. All subsequent cycles were executed under the same conditions with a denaturation step of 30 sec instead of 2.5 min. In the last RT-PCR cycle, the elongation step was extended to 8 min. After RT-PCR, 15 μ l of individual RT-PCR product and 5 μ l of xylene band-loading buffer were electrophoresed in 1.5% agarose gel in TAE buffer. The correct RT-PCR product band size was analyzed and verified with corresponding bands in a 100-base pair (bp) DNA ladder (Promega). The gel

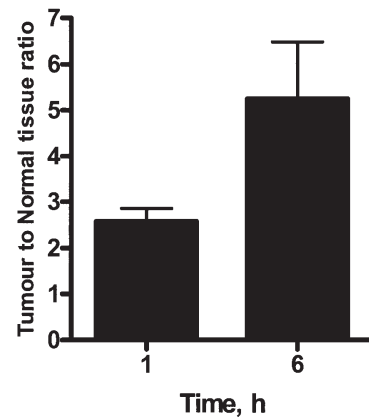


Figure 3. Tumor to normal tissue ratio at 1 and 6 h after administration of hypericin. Each group represents the mean (bars, SE) of five tumors.

was viewed and captured as a digital image by the Gel Documentation System (Bio-Rad Laboratories). Semi-quantitative measurements were derived by expressing the RT-PCR fragment's band intensity ratio with the gene of interest against glyceraldehyde-3-phosphate dehydrogenase (GAPDH).

Statistical analysis. Statistical analysis was performed using GraphPad Prism, version 4.0 (GraphPad Software, Inc., San Diego, CA). One-way ANOVA was used to analyse the variance, and Dunnett's Multiple Comparison test was used to compare the VEGF levels in all the groups. The non-parametric Mann-Whitney test was used to compare the human VEGF levels in the PDT and celebrex treatment groups. A p-value of <0.05 was considered to be significant.

Results

Fluorescence distribution in normal and tumor tissue. Fluorescence intensity in the nasopharyngeal xenografts was higher at 6 h compared to 1 h post hypericin administration. Greater fluorescence was observed in the macroscopic images of tumor, skin and muscle at 6 h post hypericin administration compared to the 1-h images. (Fig. 2a). The red color in the enhanced image was the fluorescence exhibited by the accumulated hypericin (Fig. 2b). The tumor to normal tissue ratio tabulated from the fluorescence images was greater at 6 h compared to 1 h post hypericin administration (Fig. 3).

Mouse and human VEGF in serum. Both mouse and human VEGF were estimated for this study as human nasopharyngeal carcinoma xenografts were induced in a mouse model. The control groups were animals with untreated nasopharyngeal carcinoma xenografts. The treated tumors were extracted at 24, 48 and 72 h in order to investigate the immediate PDT effect on the VEGF levels and also to understand the role of VEGF in tumor regrowth post PDT. The mouse VEGF in serum decreased at 24 and 48 h post treatment compared to the control group. However, at 72 h post PDT the mouse VEGF levels increased in the treatment groups and were comparable to the control group. The difference in the concentration of mouse VEGF in the various

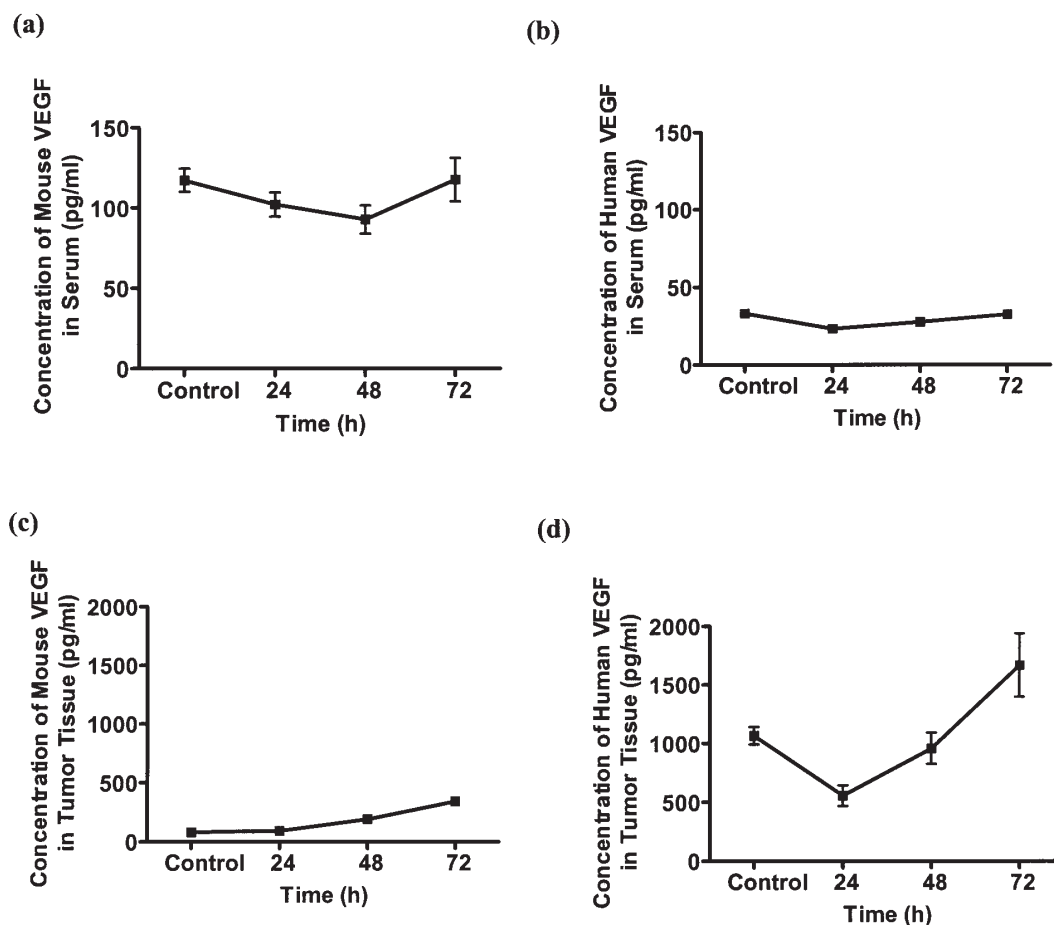


Figure 4. Concentration of (a) mouse VEGF in serum; (b) human VEGF in serum; (c) mouse VEGF in tumor tissue; and (d) human VEGF in tumor tissue at different time points post hypericin-PDT. Each group represents the mean (bars, SE) of eight tumors.

Table I. The sequence, expected fragment size and primers used in the semi-quantitative RT-PCR analysis to study the mRNA expression of VEGF-A.

Gene	Sequence	Expected fragment size	Gene Bank acc. no.	Description
VEGF A	Forward 5' tcc agg agt acc ctg atg ag 3' Reverse 5' ctt tcc tgg tga gag atc tgg 3'	457 (VEGF A 165) 303 (VEGF A 121)	AF 023375	<i>Homo sapiens</i> vascular endothelial growth factor

PDT groups and the control group was not statistically significant ($p > 0.05$) (Fig. 4a).

A similar trend was observed in the expression of human VEGF in the serum. At 24 and 48 h the VEGF levels were downregulated, but at 72 h the VEGF levels reached control levels suggesting that regrowth in the tumor begins as early as 72 h post hypericin-PDT. However, the difference in VEGF concentration compared to the control group was found to be statistically significant in the 24-h post-PDT group only ($p < 0.05$) (Fig. 4b).

Mouse and human VEGF in tumor tissue. A higher concentration of VEGF was observed in the tumor tissue than in the serum. Mouse and human VEGF were significantly higher in the tumor tissue (320-1700 pg/ml) compared to serum (33-110 pg/ml). Mouse VEGF in tumor tissue

increased at 48 and 72 h post PDT. The difference in mouse VEGF concentration in the control and the 72-h post-PDT group was found to be statistically significant suggesting that regrowth could have started as early as 3 days after hypericin-PDT (Fig. 4c). Similar trends were observed in human VEGF in the nasopharyngeal xenograft tissue where VEGF levels were downregulated immediately after PDT but were above control levels within the next 3 days post PDT. The increase in VEGF levels from 24 to 72 h was found to be statistically significant ($p < 0.05$) (Fig. 4d). Controls in our experiments were animals with untreated tumors.

Effect of anti-angiogenesis treatment with celebrex on VEGF expression. At 24 days post hypericin PDT, VEGF levels in serum increased to ~240 pg/ml. In the control and celebrex only group, VEGF levels were at 135 pg/ml, and lower

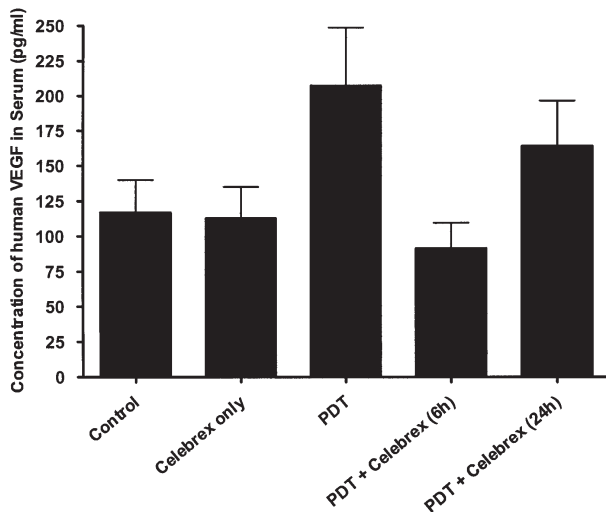


Figure 5. Concentration of human VEGF in various treatment groups was measured 24 days post PDT. For the PDT + celebrex treatment, initial administration of celebrex was at 6 h post PDT for one group and at 24 h post PDT for the other group. Each group represents mean (bars, SE) of five animals.

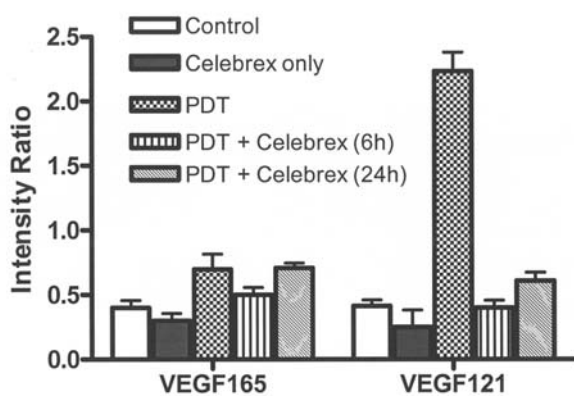


Figure 6. mRNA gene expression of VEGF 165 and 121 in various treatment groups. Each group represents mean (bar, SE) of five tumors.

human VEGF levels (110 pg/ml) were observed in the PDT and celebrex group when the initial dose of celebrex was administered at 6 h post hypericin-PDT. However, when the initial dose of celebrex was administered 24 h post hypericin-PDT, VEGF was upregulated at 190 pg/ml. This indicates that the timing of administration of the anti-angiogenesis agents post PDT is an important factor in the tumor regrowth process (Fig. 5).

Expression of VEGF A 121 and 165 genes. VEGF A isoforms 121 and 165 were upregulated in the nasopharyngeal tumor tissue post hypericin-mediated PDT. Tumors treated with celebrex from 6 h post PDT exhibited significant down-regulation of both VEGF A 121 and 165 (Fig. 6). The gene sequence for the isomers is shown in Table I.

Discussion

Nasopharyngeal carcinoma (NPC) is an epithelial tumor seen mostly in Southern Chinese and Southeast Asian populations.

Chemotherapy and radiotherapy are being currently used to treat early NPC tumors. However, effective treatment is lacking for recurrent or residual tumors. In such cases, photodynamic therapy has shown promise as an alternative treatment modality (12). In this study an attempt has been made to understand the initiation of regrowth in nasopharyngeal carcinoma xenograft tumors post hypericin-mediated PDT by assessing the expression of angiogenesis promoter, vascular endothelial growth factor (VEGF).

The use of appropriate drug and light dosimetry and the time interval between drug and light administration can greatly affect the outcome of PDT. We have previously shown the depth of necrosis to be 4.5 mm from the surface of the skin in hypericin-PDT treated tumors at the wavelength region of 560-640 nm (20). To determine the optimal drug-light interval for treatment, the tumor to normal ratio was assessed at 1 h and 6 h post hypericin administration based on previous hypericin uptake studies (21). As the drug started to clear from the normal regions, the tumor to normal tissue ratio was found to be higher at 6 h post hypericin administration, and also the intratumoral accumulation of hypericin was found to be maximal at this time point. Therefore the 6-h drug-light interval was maintained throughout the experiments to optimally treat the tumors without damaging the normal tissue.

Photodynamic therapy with hypericin has shown to induce an acute and potent vascular effect that is responsible for tumor destruction. Studies have also indicated that tumor vasculature damage occurs due to resultant oxygen and nutrient deprivation (22). The consumption of oxygen during PDT as well as the damage to the tumor microvasculature causes oxygen shortage within the treated tumor (1). The hypoxic condition in the tumor tissue triggers the hypoxia-inducible factor (HIF-1 α) as a stress response thereby promoting certain angiogenesis growth factors including VEGF (23). Earlier studies have reported that hypoxia plays a major role in the expression of VEGF in tumor tissue (24). It has also been reported that PDT produced significant increases in VEGF within treated lesions (25). The expression of VEGF in areas surrounding tumor necrosis has also indicated that hypoxia within tumors plays a major role in angiogenesis (26,27).

Angiogenesis is a normal process in growth and development, as well as in wound healing. However, angiogenesis is also an essential step in the transition of a small cluster of mutated cells to a larger malignant tumor. *In vitro* studies have clearly demonstrated that VEGF is a potent mediator of angiogenesis as it helps in the proliferation and migration of the endothelial cells to form tube-like capillaries (28). Our initial studies have shown that photodynamic therapy has a significant effect on the expression profile of VEGF. In order to understand the initiation of regrowth post hypericin-PDT, we compared the VEGF levels at 24, 48 and 72 h after treatment. VEGF levels were estimated for only 3 days post PDT as we were interested in investigating the immediate effects of PDT. Controls in our experiments were animals with untreated tumors. As we used human nasopharyngeal carcinoma cells as xenografts in a mouse model, both human and mouse VEGF were estimated in serum and in the tumor. The decrease in mouse VEGF in serum immediately post



was not significant, but it reached control levels at 72 h. A greater amount of mouse VEGF compared to human VEGF in serum could indicate the involvement of the host environment in modulating the PDT response of the tumor. Also, a greater amount of human VEGF in the tumor itself demonstrates that the treated nasopharyngeal carcinoma cells expressed most of the detectable human VEGF.

At 24 h post PDT, both the mouse and human VEGF levels in tumor tissue decreased compared to the control group but were elevated by 72 h. The decrease in VEGF observed at 24 h post PDT may be explained by postulating that the residual tumor cells from the initial PDT treatment could be reoxygenated after 24 h following PDT (29) or may be due to the reversal of temporary vascular occlusion (30). Down-regulation of VEGF immediately after PDT and its subsequent upregulation at 72 h indicates that regrowth in tumors after PDT begins as early as 72 h. It can be argued that both tumor angiogenesis and recurrence may therefore be mediated by PDT via the enhancement of VEGF expression within the treated tumor mass (25).

Mouse VEGF levels were found to be significantly lower than human VEGF in the tumor tissue and this may be attributed to the number of host cells versus the number of tumor cells present within the treated region. Similar observations were reported by Gomer *et al* (31). Detection of VEGF has long been known as a potential serum diagnostic marker for malignant diseases. Increased serum VEGF concentrations have been measured in various types of cancer, including brain, lung, renal and ovarian (32). High serum VEGF has been strongly associated with poor clinical outcome in lymphoma patients (33). Overexpression of VEGF is known to be common in NPC, which is related to hypoxia upregulated expression involving a HIF-dependent pathway, and is associated with poor prognosis. Targeting the hypoxia pathway may be useful in the treatment of NPC (34). Patients with nasopharyngeal carcinoma having high VEGF levels in serum have been associated with a worse progression-free survival. A recent study has also shown an increased microvessel density in oral cancer tissues in VEGF-positive tumors and has indicated that upregulation of VEGF was correlated with tumor angiogenesis and disease progression (35).

Celebrex, a COX-2 inhibitor was used along with hypericin-PDT to investigate its role in the expression of VEGF. Lower levels of VEGF compared to control tumors were detected when an initial dose of celebrex was administered 6 h post hypericin-PDT. VEGF has been associated with the upregulation of COX-2 expression in endothelial cells (36). This suggests that celebrex is involved in disrupting certain critical angiogenesis pathways that play a role in the expression of VEGF. It has also been reported that celebrex inhibits tumor proliferation in the presence or absence of COX-2 expression (37). Therefore, the development of agents targeting tumor angiogenesis may be an effective strategy to control and treat various malignancies (38,39), and the administration of the initial dose of anti-angiogenesis inhibitor also seems to play a major role in tumor growth suppression.

The isoforms VEGF 121, VEGF 165 and VEGF 189 appear to be preferentially expressed by most of the VEGF-producing cells. It has been reported that VEGF 165 and

VEGF 189 were detected in higher concentrations in colorectal tumors than in normal tissue (40). In our study the expression of genes VEGF A 165 and VEGF A 121 was suppressed when COX-2 inhibitor celebrex was combined with PDT. The VEGF genes were more efficiently controlled when celebrex was administered from 6 h post PDT compared to the initial administration at 24 h post PDT, suggesting that certain important molecular pathways can be targeted and blocked immediately post PDT in order to achieve greater tumor control.

In conclusion, VEGF is upregulated after hypericin-mediated PDT due to hypoxic conditions. Also, VEGF acts as a potent angiogenesis stimulating factor that has potential as a tumor biomarker to determine the outcome of photodynamic therapy. Therefore, combining anti-angiogenesis inhibitors along with hypericin-mediated PDT, especially to target the VEGF pathway, leads to greater efficacy in nasopharyngeal cancer treatment.

Acknowledgements

The authors would like to thank the National Medical Research Council (NMRC) Singapore for funding the project and the National Cancer Centre Singapore, where the research study was carried out. We also thank Dr Mac Ho Meng Fatt for his valuable suggestions.

References

1. Dougherty TJ, Gomer CJ and Henderson BW: Photodynamic therapy. *J Natl Cancer Inst* 90: 889-905, 1998.
2. Triesscheijn M, Baas P, Schellens JH and Stewart FA: Photodynamic therapy in oncology. *Oncologist* 11: 1034-1044, 2006.
3. Kiesslich T, Krammer B and Plaetzer K: Cellular mechanisms and prospective applications of hypericin in photodynamic therapy. *Curr Med Chem* 13: 2189-2204, 2006.
4. Chen B and de Witte PA: Photodynamic therapy efficacy and tissue distribution of hypericin in a mouse P388 lymphoma tumor model. *Cancer Lett* 150: 111-117, 2000.
5. Olivo M, Lau W, Manivasager V, Bhuvanewari R, Wei Z, Soo KC, Cheng C and Tan PH: Novel photodynamic diagnosis of bladder cancer: *Ex vivo* fluorescence cytology using hypericin. *Int J Oncol* 23: 1501-1504, 2003.
6. Henderson BW, Gollnick SO, Snyder JW, Busch TM, Kousis PC, Cheney RT and Morgan J: Choice of oxygen-conserving treatment regimen determines the inflammatory response and outcome of photodynamic therapy of tumors. *Cancer Res* 64: 2120-2126, 2004.
7. Folkman J: Anti-angiogenesis: new concept for therapy of solid tumors. *Ann Surg* 175: 409-416, 1972.
8. Ferrara N: Vascular endothelial growth factor as a target for anticancer therapy. *Oncologist* 9: 2-10, 2004.
9. Pugh CW and Ratcliffe PJ: Regulation of angiogenesis by hypoxia: Role of the HIF system. *Nat Med* 9: 677-684, 2003.
10. Giles FJ: The vascular endothelial growth factor (VEGF) signaling pathway: a therapeutic target in patients with hematologic malignancies. *Oncologist* 6: 32-39, 2001.
11. Lee AW, Sze WM, Au JS, Lee AW, Sze WM, Au JS, Leung SF, Leung TW, Chua DT, Zee BC, Law SC, Teo PM, Tung SY, Kwong DL and Lau WH: Treatment results for nasopharyngeal carcinoma in the modern era: the Hong Kong experience. *Int J Radiat Oncol Biol Phys* 61: 1107-1116, 2005.
12. Wiwanitkit V: Photodynamic therapy for nasopharyngeal cancer. *Cancer Ther* 3: 321-324, 2005.
13. Krishna SM, James S and Balam P: Expression of VEGF as prognosticator in primary nasopharyngeal cancer and its relation to EBV status. *Virus Res* 115: 85-90, 2006.
14. Zhao GQ, Xu Y and Wang Q: Significance of serum vascular endothelial growth factor test before radiotherapy in patients with nasopharyngeal carcinoma. *Zhong Xi Yi Jie He Xue Bao* 3: 274-277, 2005.

15. Herbst RS: Therapeutic options to target angiogenesis in human malignancies. *Expert Opin Emerg Drugs* 11: 635-650, 2006.
16. Solban N, Selbo PK, Sinha AK, Chang SK and Hasan T: Mechanistic investigation and implications of photodynamic therapy induction of vascular endothelial growth factor in prostate cancer. *Cancer Res* 66: 5633-5640, 2006.
17. Yee KK, Soo KC and Olivo M: Anti-angiogenic effects of hypericin-photodynamic therapy in combination with celebrex in the treatment of human nasopharyngeal carcinoma. *Int J Mol Med* 16: 993-1002, 2005.
18. Zhou Q, Olivo M, Lye KY, Moore S, Sharma A and Chowbay B: Enhancing the therapeutic responsiveness of photodynamic therapy with the antiangiogenic agents SU5416 and SU6668 in murine nasopharyngeal carcinoma models. *Cancer Chemother Pharmacol* 56: 569-577, 2004.
19. Zheng W, Olivo M and Soo KC: The use of digitized endoscopic imaging of 5-ALA-induced PPIX fluorescence to detect and diagnose oral premalignant and malignant lesions *in vivo*. *Int J Cancer* 110: 295-300, 2004.
20. Thong PS, Watt F, Ren MQ, Tan PH, Soo KC and Olivo M: Hypericin-photodynamic therapy (PDT) using an alternative treatment regime suitable for multi-fraction PDT. *J Photochem Photobiol B* 82: 1-8, 2006.
21. Du HY, Bay BH and Olivo M: Biodistribution and photodynamic therapy with hypericin in a human NPC murine tumor model. *Int J Oncol* 22: 1019-1024, 2003.
22. Chen B, Roskams T, Xu Y, Agostinis P and DeWitte PA: Photodynamic therapy with hypericin induces vascular damage and apoptosis in the RIF-1 mouse tumor model. *Int J Cancer* 98: 284-290, 2002.
23. Richard DE, Berra E and Pouyssegur J: Angiogenesis: How a tumor adapts to hypoxia. *Biochem Biophys Res Commun* 266: 718-722, 1999.
24. Robbins SG, Conaway JR, Ford BL, Roberto KA and Penn JS: Detection of vascular endothelial growth factor (VEGF) protein in vascular and non-vascular cells of the normal and oxygen-injured rat retina. *Growth Factors* 14: 229-241, 1997.
25. Ferrario A and Gomer CJ: Avastin enhances photodynamic therapy treatment of Kaposi's sarcoma in a mouse tumor model. *J Environ Pathol Toxicol Oncol* 25: 251-259, 2006.
26. Shweiki D, Itin A, Soffer D and Keshet E: Vascular endothelial growth factor induced by hypoxia may mediate hypoxia-initiated angiogenesis. *Nature* 359: 843-845, 1992.
27. Senger DR, Perruzzi CA, Feder J and Dvorak HF: A highly conserved vascular permeability factor secreted by a variety of human and rodent tumor cell lines. *Cancer Res* 46: 5629-5632, 1986.
28. Bernatchez PN, Soker S and Sirois MG: Vascular endothelial growth factor effect on endothelial cell proliferation, migration, and platelet-activating factor synthesis is Flk-1-dependent. *J Biol Chem* 274: 31047-31054, 1999.
29. Uehara M, Inokuchi T, Sano K and Zuolin W: Expression of vascular endothelial growth factor in mouse tumors subjected to photodynamic therapy. *Eur J Cancer* 37: 2111-2115, 2001.
30. Tsutsui H, MacRobert AJ, Curnow A, Rogowska A, Buonaccorsi G, Kato H and Bown S: Optimisation of illumination for photodynamic therapy with mTHPC on normal colon and a transplantable tumor in rats. *Lasers Med Sci* 17: 101-109, 2002.
31. Gomer CJ, Ferrario A, Luna M, Rucker N and Wong S: Photodynamic therapy: combined modality approaches targeting the tumor microenvironment. *Lasers Surg Med* 38: 516-521, 2006.
32. Kondo S, Asano M, Matsuo K, Ohmori I and Suzuki H: Vascular endothelial growth factor/vascular permeability factor is detectable in the sera of tumor-bearing mice and cancer patients. *Biochim Biophys Acta* 1221: 211-214, 1994.
33. Salven P, Orpana A, Teerenhovi L and Joensuu H: Simultaneous elevation in the serum concentrations of the angiogenic growth factors VEGF and bFGF is an independent predictor of poor prognosis in non-Hodgkin lymphoma: a single-institution study of 200 patients. *Blood* 96: 3712-3718, 2000.
34. Hui EP, Chan AT, Pezzella F, Turley H, To KF, Poon TC, Zee B, Mo F, Teo PM, Huang DP, Gatter KC, Johnson PJ and Harris AL: Coexpression of hypoxia-inducible factors 1alpha and 2alpha, carbonic anhydrase IX, and vascular endothelial growth factor in nasopharyngeal carcinoma and relationship to survival. *Clin Cancer Res* 8: 2595-2604, 2002.
35. Shang ZJ, Li JR and Li ZB: Upregulation of serum and tissue vascular endothelial growth factor correlates with angiogenesis and prognosis of oral squamous cell carcinoma. *J Oral Maxillofac Surg* 65: 17-21, 2007.
36. Wu G, Mannam AP, Wu J, Kirbis S, Shie JL, Chen C, Laham RJ, Sellke FW and Li J: Hypoxia induces myocyte-dependent COX-2 regulation in endothelial cells: role of VEGF. *Am J Physiol Heart Circ Physiol* 285: H2420-H2429, 2003.
37. Waskewich C, Blumenthal RD, Li H, Stein R, Goldenberg DM and Burton J: Celecoxib exhibits the greatest potency amongst cyclooxygenase (COX) inhibitors for growth inhibition of COX-2 negative hematopoietic and epithelial cell lines. *Cancer Res* 62: 2029-2033, 2002.
38. Oh SH, Kim WY, Kim JH, Younes MN, El-Naggar AK, Myers JN, Kies M, Cohen P, Khuri F, Hong WK and Lee HY: Identification of insulin-like growth factor binding protein-3 as a farnesyl transferase inhibitor SCH66336-induced negative regulator of angiogenesis in head and neck squamous cell carcinoma. *Clin Cancer Res* 12: 653-661, 2006.
39. Fox BS: Angiogenesis: pathological, prognostic, and growth-factor pathways and their link to trial design and anticancer drugs. *Lancet Oncol* 2: 278-289, 2001.
40. Cressey R, Wattananupong O, Lertprasertsuke N and Vinitketkumnuen U: Alteration of protein expression pattern of vascular endothelial growth factor (VEGF) from soluble to cell-associated isoform during tumorigenesis. *BMC Cancer* 5: 128, 2005.